

UC San Diego

UC San Diego Previously Published Works

Title

Shear strength behavior of clayey soil reinforced with polypropylene fibers under drained and undrained conditions

Permalink

<https://escholarship.org/uc/item/4p4695qr>

Journal

Geotextiles and Geomembranes, 49(5)

ISSN

0266-1144

Authors

Correia, NS
Rocha, SA
Lodi, PC
[et al.](#)

Publication Date

2021-10-01

DOI

10.1016/j.geotexmem.2021.05.005

Peer reviewed

1 Shear strength behavior of clayey soil reinforced with polypropylene 2 fibers under drained and undrained conditions

3
4
5
6
7
8 N. S. Correia ^{a, *}, S. A. Rocha ^b, P. C. Lodi ^c, J. S. McCartney ^d
9

10
11
12
13 ^{a, b} UFSCar - Federal University of Sao Carlos, Department of Civil Engineering (SP),
14 Brazil
15

16
17
18 ^c UNESP - São Paulo State University, School of Engineering at Bauru (SP), Brazil
19

20
21 ^d UCSD – University of California at San Diego (CA), USA
22

23
24
25 * Corresponding author (N. S. Correia); tel: (+55 16 98802 6709)
26

27
28 UFSCar - Federal University of Sao Carlos, Department of Civil Engineering
29

30
31 Washington Luis Road, km 235, Sao Carlos, SP, Brazil, e-mail: ncorreia@ufscar.br,
32

33
34 E-mail addresses: ncorreia@ufscar.br (N.S. Correia), sabrina-andrade@outlook.com (S.
35

36
37 A. Rocha), paulo.lodi@unesp.br (P.C. Lodi), mccartney@ucsd.edu (J.S. McCartney)
38

39
40
41
42
43
44
45
46
47
48
49
50
51
52
53
54
55
56
57
58
59
60
61
62
63
64
65
ABSTRACT: The use of fiber reinforcement has been recognized as a viable soil improvement technique in numerous fill-type geotechnical applications. However, fewer studies on the use of fiber reinforcement in clayey soil have been reported compared to those in sandy soils despite equal potential for application in practice. The fundamental mechanisms controlling shear strength and deformability behavior of clay-fiber mixtures have still not been well established, nor the constraints that may affect their performance of shearing under different drainage conditions. This study aims to understand the behavior of a clay soil mixed with polypropylene fibers using results from drained and undrained triaxial compression tests, and to provide necessary calibration data for a shear strength prediction model. In drained tests, shear strength increased with fiber inclusion

26 for a given mean effective stress, represented by an increase in apparent cohesion. In the
27 undrained tests, the shear strength was not affected by pore water pressure generation.
28 Results from the drained and undrained tests indicate that the fiber content had a greater
29 influence on the apparent cohesion than on the friction angle. Drainage affected
30 improvement in the shear strength of fiber-reinforced soils, with similar improvement in
31 the drained and undrained tests for higher confining stresses.

32
33 **KEYWORDS:** Polypropylene fibers; Clayey soil; Fiber reinforcement model, Triaxial
34 compression; Drainage.

35 36 1. Introduction

37 Fiber reinforcement is an established approach to improve the shear strength and
38 ductility of the stress-strain response of soils. In particular, the use of fiber reinforcement
39 to permit the use of poorly draining, locally-available soils has gained increased attention
40 and acceptance (Abou Diab et al. 2018; Hejazi et al. 2012; Sadek et al. 2010). Examples
41 of applications where fiber-reinforced soils have been used in geotechnical engineering
42 include retaining structures, stabilization of subgrade and subbases, improvement in soil
43 bearing capacity, slope stability, soft soil embankments, controlling soil hydraulic
44 conductivity, erosion improvement, piping prevention and mitigation of shrinkage cracks
45 (Ehrlich et al. 2019; Shukla 2017; Tang et al. 2007; Ziegler et al. 1998).

46 Several authors have investigated the behavior of fiber-reinforced sands and found that
47 inclusions of fibers improve the mechanical response of soils by mobilizing the tensile
48 strength of fibers intersecting shear failure planes in the soil, resulting in a greater shear
49 strength and an improvement in soil ductility (Gray 1986; Santoni et al., 2001; Consoli et
50 al., 2002; Velloso et al., 2010; Sotomayor and Casagrande 2018; Louzada et al. 2019).

1
2
3
4
5
6
7
8
9
10
11
12
13
14
15
16
17
18
19
20
21
22
23
24
25
26
27
28
29
30
31
32
33
34
35
36
37
38
39
40
41
42
43
44
45
46
47
48
49
50
51 Fewer studies have investigated clay-fiber mixtures despite equal potential for application
52 in geotechnical practice. The limited number of studies on fiber-reinforced clays have not
53 yet established the fundamental mechanisms involving the behavior of clayey-fiber
54 mixtures or the conditions that may affect their performance (Anagnostopoulos et al.
55 2013). In particular, only a few studies have focused on the shear strength of soil-fiber
56 mixtures under undrained conditions, with most of these studies indicating that further
57 research is necessary on this topic (e.g., Freilich et al. 2010; Li and Zornberg 2013;
58 Mirzababaei et al. 2018).

59 Feuerhemel (2000) studied the inclusion of PP fibers (lengths of 12 and 36 mm and
60 mixture of 0.50% fibers by volume) in a clayey soil using consolidated drained (CD)
61 triaxial compression tests. Results showed a continuously increasing stress-strain curve
62 with high ductility. Inclusion of fibers was found to increase the apparent cohesion by 3
63 times (fiber length of 12 mm) to 5 times (fiber length of 36 mm), while the friction angle
64 was unaffected. Trindade et al. (2006) also evaluated the inclusion of PP fibers (20 mm
65 and 0.25%) in a clayey soil using CD triaxial tests and showed that fibers reduced soil
66 compressibility, while the friction angle remained unchanged, and the apparent cohesion
67 increased by up to 70%.

68 Freilich et al. (2010) observed that the effective shear strength parameters of soil-PP
69 fibers from consolidated undrained (CU) triaxial compression tests were greater than
70 from drained conditions, evidencing that the effective strength of the mixture may
71 significantly decrease with time and drainage. Li (2005) noted that competing factors may
72 arise in the fiber-soil interaction mechanism in clays, such as volume change tendency of
73 soil and strain rate. Li (2005) also noted that the pore water pressure values at the fiber-
74 soil interfaces within a specimen may differ from the pore water pressure measured at the
75 ends of a clay specimens in a triaxial test. Özkul and Baykal (2007) also conducted CU

1
2
3
4
5
6
7
8
9
10
11
12
13
14
15
16
17
18
19
20
21
22
23
24
25
26
27
28
29
30
31
32
33
34
35
36
37
38
39
40
41
42
43
44
45
46
47
48
49
50
51
52
53
54
55
56
57
58
59
60
61
62
63
64
65

76 and CD triaxial tests with 25 mm tire fibers in a clayey soil and found that the apparent
77 cohesion values of the fiber-clay from CD triaxial tests were lower than those from CU
78 triaxial tests. However, the friction angles from the tests with different drainage
79 conditions were the same. Louzada et al. (2019) evaluated the mechanical behavior of a
80 clayey soil mixed with PET flakes using CD triaxial tests and observed that an increasing
81 flake content improved the interaction with soil particles, with an increasing trend in
82 improvement with increasing effective confining stress.

83 Murray et al. (2000) found that adding 1% PP virgin polypropylene fibers to sandy
84 silty soil in CU triaxial tests led to an increase in the undrained shear strength with a more
85 ductile post-peak response. Khatri et al. (2016) also carried out a series of CU triaxial
86 tests on fiber-reinforced clay and reported improved undrained shear strength with the
87 increase in coir fiber content from 0.4% to 1.6%. Mirzababaei et al. (2017) evaluated the
88 inclusion of recycled carpet fibers in a clayey soil using CU triaxial tests. The fiber
89 content of 3% presented higher shear strength at the initial mean effective stress of 50
90 kPa when compared to the soil with 5% fiber. According to Mirzababaei et al. (2017), an
91 increase in fiber content at a low initial effective consolidation stress may have an adverse
92 effect on the strength of the reinforced soil by affecting soil grain interaction. Suffri et al.
93 (2019) evaluated a clayey soil with coir fiber contents of 0.5 to 2.0% using CU triaxial
94 tests and found that the inclusion of fibers increased the undrained shear strength.
95 Mirzababaei et al. (2020) evaluated the reorientation of fibers in miniature fiber-
96 reinforcement clay samples during unconsolidated undrained (UU) triaxial tests using
97 computed tomography (CT) imaging. The results indicate that compaction induces an
98 anisotropic distribution, and that fibers accumulated in the lower part of the specimens,
99 with most fibers aligning in the horizontal direction. Palat et al. (2019) conducted CU
100 triaxial tests in fiber-clay soils and emphasize that no conclusion could be made on the

101 development of pore water pressure by the inclusion of fibers, and that more tests are
102 necessary.

103 Jamei et al. (2013) developed an analytical method for predicting the undrained shear
104 strength of fiber-clays for short-term stability analyses. The model of Jamei et al. (2013)
105 is an extension of the model of Michalowski and Zhao (1996) for fiber-reinforced sands,
106 and was developed to predict the principal stresses at failure for clayey soil-fibers
107 mixtures as a function of volumetric fiber content, length, diameter, apparent cohesion
108 and friction angle of the clay, and interface shear strength parameters. However,
109 information on the interface shear strength parameters has been still an issue in
110 quantifying the effectiveness of fiber-clay shear strength predictions using this model. To
111 address the issues raised in the literature review, this study aims to understand the
112 behavior of a clayey soil mixed with recycled polypropylene fibers using results from
113 drained and undrained triaxial compression tests. The model of Jamei et al. (2013) was
114 then used to capture the variations in undrained shear strength of fiber-reinforced clays
115 with different relevant variables for this soil and for the clays investigated in the other
116 studies mentioned in this section.

117

118 2. Experimental Program

119 2.1. Materials

120 The soil used in this research was obtained from the city of Santa Gertrudes, Sao Paulo -
121 Brazil and is representative of residual soils that cover a large area of this territory. The
122 clayey soil has a clay fraction of 50%, a silt fraction of 14%, and a sand fraction of 36%
123 (ASTM D7928-17). According to an X-ray diffraction analysis (ASTM D4452-14), the
124 clay fraction in the soil has predominant clay minerals of kaolinite, illite and hematite,
125 while the silt and sand fraction is primarily quartz. The specific gravity of solids was

126 found to be 2.9 (ASTM D854-14). The fines fraction of the clayey soil has a liquid limit
127 of 51, a plastic limit of 29, and a plasticity index of 22 (ASTM D4318), so it classifies as
128 a CH clay according to the Unified Soil Classification Scheme (ASTM D2487-17). Short
129 discrete recycled polypropylene (PP) fibers were used as the reinforcements in this study.
130 The PP-fibers have an average diameter (d_f) of 18 micrometers, a specific gravity (G_f) of
131 0.9, an average length (L_f) of 12 mm, zero water absorption, and a breaking tensile
132 strength of 610 MPa.

133

134 2.2. *Specimen Preparation*

135 A fiber content of 0.25% was selected for the experiments in this study as it is
136 representative of soil mixtures evaluated in other studies (Feuerharmel 2000; Li and
137 Zornberg 2005; Özkul and Baykal 2007; Freilich et al., 2010; Rowland Otoko 2014;
138 Diambra and Ibraim 2014; Mirzababaei et al. 2017). Greater fiber contents were
139 evaluated, but issues with homogenization occurred, so only a single fiber content was
140 investigated in this study to demonstrate the impacts of drainage conditions on the shear
141 strength of fiber reinforced soils. Before mixing the fibers, the soil was homogenized to
142 different initial gravimetric water contents. Then, PP fibers were randomly distributed in
143 the soil matrix and a mechanical mixer was used to reach a homogenous distribution of
144 fibers in the soil. To obtain the target compaction parameters for the soil-fiber mixture,
145 standard Proctor compaction tests were conducted on the soil with and without fiber
146 reinforcements according to ASTM D698-12e2. Prior to compaction, prepared mixtures
147 were preserved in sealed bags for a minimum of 24 hours for moisture homogenization.
148 The standard Proctor compaction curves for the clay with and without fiber
149 reinforcements are shown in Figure 1. Although there are slight differences, it can be
150 assumed that the presence of fibers does not significantly alter the compaction curve for

151 the soil, and the compaction curve for the unreinforced soil was used as the reference for
152 specimen preparation. Results of other studies show similar compaction curves for soils
153 with and without fiber reinforcement (Kumar and Singh 2008; Mirzababaei et al. 2013;
154 Gelder and Fowmes 2016).

155 2.3. Triaxial Test Procedures

156 In order to investigate the shear strength behavior of soil-fiber mixtures, triaxial
157 consolidated-drained (CD) and consolidated-undrained (CU) tests were performed on the
158 soil-fiber mixtures according to ASTM D7181-20 and ASTM D4767-20, respectively.
159 The 50 mm-diameter specimens were statically compacted to a height of 100 mm to reach
160 as relative compaction of 95% at the optimum gravimetric water content of the
161 unreinforced soil. The specimens were saturated using water percolation and
162 backpressure, and a minimum B-parameter of 0.9 (Skempton 1954) was reached in each
163 test. Subsequently, specimens were consolidated mean effective stresses of 50, 100, 200,
164 and 300 kPa, which are within the range of stresses investigated in previous studies (e.g.,
165 Freilich et al., 2010; Mirzababaei et al., 2017; Özkul and Baykal, 2007). The shearing rate
166 was set to be 0.01 mm/min in the CD triaxial tests and 0.15 mm/min in the CU triaxial
167 tests.

169 3. Test Results

170 3.1. Triaxial Test Results

171 Deviator stress-axial strain and volumetric strain-axial strain curves for specimens
172 with fiber contents of 0 and 0.25% from isotropic CD triaxial compression tests are shown
173 in Figure 2. As expected, an increase in shear strength and an increase in contraction are
174 observed with increasing mean effective stresses for both materials. After a fiber-clay
175 mixture undergoes plastic deformation, the resistance of the fibers is mobilized, and

176 hardening is observed. For the higher mean effective stresses, the fiber-clay mixtures
177 showed a hardening behavior and did not exhibit a clear peak shear strength. This
178 behavior was also observed by Feuerhemel (2000). Regarding the volumetric strain-axial
179 strain response, the clay-fiber mixtures showed greater contraction than the clay with no
180 fiber reinforcement. Greater contraction during shearing of fiber-reinforced soils
181 compared with unreinforced soils was also observed by Abou Diab et al. (2018) and
182 Louzada et al. (2019). In addition, all specimens exhibited bulging behavior after
183 shearing, which, according to Özkul and Baykal (2007) and Ekinici and Ferreira (2012),
184 is a typical behavior of fiber-clay samples. As observed in the study of Abou Diab et al.
185 (2018) and herein, the addition of fiber reinforcements reduced the degree of bulging and
186 resulted in a uniform deformation along the length of the specimens.

187 The relationships between the secant elastic modulus with axial strain and between the
188 principal effective stress ratio (σ_1'/σ_3') and the axial strain for clayey soils with and
189 without reinforcement are shown in Figures 3a and 3b, respectively. A greater modulus
190 is observed for the reinforced soil in comparison with the unreinforced soil, especially for
191 lower mean effective stresses. The ratios in Figure 3b indicate that the efficiency of the
192 fibers does not seem to increase with the increase of the confining stresses, which is
193 expected since it improves the soil-fiber interaction. There is potentially a fiber breakage
194 effect for the higher mean effective stress levels. Mirzababaei et al. (2020) found that the
195 improvement in shear strength of fiber-reinforcement clay decreased with confining stress
196 for this reason. The fiber-clay specimens in the drained tests exhibited “bulging” behavior
197 after reaching the maximum deviator stress, and the unreinforced clay specimens
198 exhibited partial development of a shear plane. Xu et al. (2018) also observed bulging
199 failure in the CU tests with localized bulging in the middle of the specimens. Mirzababaei

200 et al. (2020) noted that bulging may occur in different vertical locations of the specimen
 201 if fibers are not uniformly distributed.

202 The stress paths for mixtures with 0% and 0.25% fiber contents are shown in Figure 4
 203 in $p' - q$ space, where q is $(\sigma_1 - \sigma_3)$ and p' is $(\sigma'_1 + 2\sigma'_3)/3$. The failure criteria adopted is
 204 the value of deviator stress at 20% of axial strain. In the drained triaxial tests, the shear
 205 strength increased with fiber inclusion for a given mean effective stress, represented by
 206 an increase in apparent cohesion. Similar behavior was observed by Trindade et al. (2006)
 207 in a study with the inclusion of 0.25% PP fibers (20 mm) in a clayey soil using CD triaxial
 208 tests. Ma et al. (2018) states that tension of fiber strengthens the bond among clay
 209 particles, which enhances the shear strength of clay.

210 The results from the CU triaxial tests are shown in Figure 5. Different from the CD
 211 triaxial tests, clear initial peak values in the deviator stress-axial strain curves are
 212 observed in Figures 5a and 5b. Although the initial peak value for the mixtures with
 213 0.25% fiber content is similar or lower than the unreinforced clay, the mixtures with
 214 0.25% fiber content show a hardening effect with continued straining. As the pore water
 215 pressures in Figures 5c and 5d show monotonically increasing trends that do not depend
 216 on the presence of fibers, the hardening effects in Figures 5a and 5b can be attributed to
 217 the fibers. A greater amount of hardening was observed for the mixtures with a fiber
 218 content of 0.25% with increasing initial mean effective stress. Similar to the results of
 219 Mirzababaei et al. (2020), higher undrained shear strengths were observed for reinforced
 220 specimens at all confining stresses.

221 The excess pore water pressures were consistently positive during the undrained
 222 triaxial tests (Fig. 5c and 5d) consistent with the trend of volume contraction observed in
 223 the drained triaxial tests. As observed in the study of Xu et al. (2018) and herein, the
 224 induced pore water pressures increased steadily with axial strain and approached an

225 asymptotic value. In general, the fibers did not influence the generation of pore water
226 pressures during undrained shearing. However, as the increase in pore water pressures led
227 to a decrease in mean effective stress, this contributed to the greater improvement in
228 deviator stress with axial strain for the tests performed at higher mean effective stresses.

229 Relationships between the secant modulus with axial strain and between the principal
230 effective stress ratio (σ_1'/σ_3') and the axial strain for clayey soils with fiber contents of 0
231 and 0.25% are shown in Figure 6a and 6b, respectively. The results in Figure 6a show
232 that there was no significant increase in the secant modulus with the inclusion of fibers,
233 while the results in Figure 6b indicate that the presence of fibers led to an improvement
234 in shear strength for higher confining stresses at consolidation.

235 Fig. 7 presents the stress paths and effective shear strength parameters (defined using
236 the maximum principal stress different failure criterion) for the clayey soil with fiber
237 contents of 0 and 0.25% from the CU triaxial tests. The effective stress paths are
238 consistent with the expected behavior of normally consolidated tropical soils (Futai et al.,
239 2004; Louzada et al., 2019). Similar to the CD triaxial test results, the presence of fibers
240 had a greater influence on the values of apparent cohesion than on the friction angle. Also
241 similar to the results from the CD triaxial tests, the effective shear strength of the fiber-
242 soil specimens was higher than the unreinforced specimens. In both drainage conditions,
243 an increase in apparent cohesion was observed without a significant effect on the friction
244 angle. The shape of the effective stress paths of unreinforced and fiber-reinforced
245 specimens reflect an increase in pore pressure with increasing strain. Different from the
246 CD triaxial tests, the effect of the fibers on the soil strength increases as the effective
247 confining pressure at consolidation increases. In other words, the tests at higher initial
248 values of p' experienced a greater change in pore water pressure, which led to less
249 interaction between the clay and fibers and a lower amount of improvement. These results

1
2
3
4
5
6
7
8
9
10
11
12
13
14
15
16
17
18
19
20
21
22
23
24
25
26
27
28
29
30
31
32
33
34
35
36
37
38
39
40
41
42
43
44
45
46
47
48
49
50
51
52
53
54
55
56
57
58
59
60
61
62
63
64
65

250 emphasize the importance of considering the clay-specific evolution in volume change
251 with strain in CD triaxial tests and pore water pressure generation with strain in CU
252 triaxial tests. The results presented herein are in agreement with the results obtained from
253 literature (Murray et al., 2000; Li, 2005; Özkul and Baykal, 2007; Freilich et al., 2010;
254 Khatri et al., 2016). Freilich et al. (2010) also observed greater shear strengths from CU
255 triaxial tests on fiber reinforced soils than from CD triaxial tests.

256 A comparison of the percent improvement in peak deviator stress as a function of the
257 confining stress at failure ($\sigma'_{3,f}$) from this study (CU and CD triaxial tests) with those
258 from the literature involving other soils and types and percentages of fibers is shown in
259 Figure 8. For the CU triaxial tests, the confining stress at failure was the same for the
260 unreinforced and reinforced soils except for the specimens tested at the highest initial
261 confining stress of 300 kPa, in which case the average confining stress at failure for the
262 reinforced and unreinforced specimens was used to create this plot. The results in this
263 figure show that drainage affected the improvement in the shear strength of fiber-
264 reinforced soils, with similar improvement in the drained and undrained tests for higher
265 confining stresses. A diminishing improvement with increasing confining stress at failure
266 was observed in both the drained and undrained tests, which was also observed by Freilich
267 et al. (2010). Studies on fiber reinforced sands indicate that extension and pullout of the
268 reinforcements may become more difficult at higher confining stresses, potentially
269 leading to fiber breakage (Li 2005; Attom and Al-Tamimi 2010; Hamidi and Hooresfand
270 2013; Najjar et al. 2013). Results of Palat et al. (2019) and Mirzababaei et al. (2018) show
271 no clear trend on the effect of confining stresses on the improvement in the undrained
272 shear strength of fiber-reinforced clayey soils.

273

274 3.2. *Predictive Model for Undrained Shear Strength of Fiber-Reinforced Clay*

275 The model of Jamei et al. (2013) was developed to capture the undrained shear strength
 276 (or principal stress difference) of fiber reinforced clay sheared under axisymmetric
 277 loading conditions. The model predicts the major principal stress at failure (σ_1) for the
 278 known minor principal stress at failure (σ_3), as follows:

$$279 \quad \sigma_1(1 + D \cdot \chi_f \cdot \tan \delta_i) - \sigma_3(-2K - D \cdot \chi_f \cdot \tan \delta_i) + \chi_f \cdot c_i(I_1 + K \cdot I_2) - B = 0 \quad (1)$$

280 where the parameters are defined as: $\chi_f = \eta_f \cdot \frac{d_f \cdot L_f^2 \cdot N_v}{2}$, $N_v = \frac{\frac{\chi_{F,v}}{100}}{\pi \left(\frac{d_f}{2}\right)^2 L_f \left(1 + \frac{\chi_{F,v}}{100}\right)}$, $\chi_{F,v} =$

$$281 \quad \frac{\eta_f \cdot \gamma_d}{(1 + \eta_f) \cdot G_f \cdot \gamma_w}, \quad K_p = \tan^2\left(45 + \frac{\phi}{2}\right), \quad K = -0.5K_p, \quad K_a = \tan^2\left(45 - \frac{\phi}{2}\right), \quad \Psi_o =$$

$$282 \quad \arctan\left(\sqrt{2K_a}\right), \quad H = -c \cdot \cot(\phi), \quad B = H(1 - K_p), \quad I_1 = \frac{\cos^3(\Psi_o)}{3}, \quad I_2 =$$

$$283 \quad \frac{3 \cdot \cos^3(\Psi_o) - \cos^3(\Psi_o)}{3}, \quad I_1'' = \frac{2 \cdot \cos^5(\Psi_o)}{5} - \frac{\cos^3(\Psi_o)}{3}, \quad I_2'' = \cos^3(\Psi_o) - \cos(\Psi_o) -$$

$$284 \quad \frac{2 \cdot \cos^3(\Psi_o)}{5} - \frac{\cos^3(\Psi_o)}{3}, \quad A' = (I_1'' + K \cdot I_2''), \quad D = (I_1 + K \cdot I_2 - A'), \quad \delta_i = C_i \cdot \tan(\phi), \quad c_i$$

285 = $C_i \cdot c$, η_f = gravimetric fiber content, d_f = equivalent fiber diameter, L_f = fiber length,

286 $\chi_{F,v}$ = volumetric fiber content; N_v = number of fibers per unit volume, γ_d = dry unit

287 weight of the clay, G_f = specific gravity of the fibers, γ_w = unit weight of the water and

288 ϕ = effective shear strength parameter of natural clay and c_i and δ_i = apparent cohesion

289 and friction angle components of interface soil-fiber strength (defined by Jamei et al.

290 2013).

291 After calculation of the major principal stress at failure, the undrained shear strength

292 can be calculated as the difference ($\sigma_1 - \sigma_3$). The parameters used in the Jamei et al. (2013)

293 predictive model are summarized in Table 1. In this study, an interface coefficient (C_i) of

294 0.8 was used to be consistent with Zornberg (2002) and Abou Diab et al. (2016). The

295 model requires the volumetric fiber content ($\chi_{F,v}$), which is equal to 0.48% for a

296 gravimetric fiber content of 0.25%.

1
2
3
4
5
6
7
8
9
10
11
12
13
14
15
16
17
18
19
20
21
22
23
24
25
26
27
28
29
30
31
32
33
34
35
36
37
38
39
40
41
42
43
44
45
46
47
48
49
50
51
52
53
54
55
56
57
58
59
60
61
62
63
64
65

297 The undrained shear strength (i.e., the maximum principal stress difference) measured
298 in the PP fiber-clay CU triaxial tests were compared with those calculated using the
299 predictive model of Jamei et al. (2013) in Figure 9. Abou Diab et al. (2016) evaluated the
300 predictive model of Jamei et al. (2013) using undrained triaxial tests of soil-fiber mixtures
301 from the literature including those of Prabakar and Sridhar (2002), Plé and Lê (2012),
302 Maheshwari et al. (2011), Jamei et al. (2013) and Wu et al. (2014), and these are also
303 included in the comparison in Figure 9 along with the data from this study. It is important
304 to highlight that a range of fiber types, contents and soils were used in this comparison.
305 For lower confining stresses, the model of Jamei et al. (2013) has a good fit to the
306 undrained shear strength data, while for higher confining stresses it tends to overestimate
307 the undrained shear strength.

309 4. Conclusions

310 This study evaluated the behavior of a clay soil mixed with recycled polypropylene
311 fibers using results from drained and undrained triaxial compression tests. Samples were
312 prepared at specified percentage of 0.25% of short fibers and were isotropically
313 consolidated under confining pressures of 50, 100, 200 and 300 kPa. The main
314 conclusions drawn from the present study are as follows:

- 315 • The experimental results of consolidated-undrained triaxial compression tests
316 show that there was improvement in the shear strength of soil with inclusion of
317 recycled PP fibers. In the drained tests, shear strength increased with inclusion of
318 recycled PP fibers for a given mean effective stress, represented by an increase in
319 apparent cohesion. Unreinforced and fiber-clay mixtures remained with similar
320 trend in volume contraction during shearing. It was found that fiber inclusions did

1
2
3
4
5
6
7
8
9
10
11
12
13
14
15
16
17
18
19
20
21
22
23
24
25
26
27
28
29
30
31
32
33
34
35
36
37
38
39
40
41
42
43
44
45
46
47
48
49
50
51
52
53
54
55
56
57
58
59
60
61
62
63
64
65

321 not mobilized stresses at low levels of strains and contributions were found to
322 occur as closer as the stress state at failure;

- 323 ● The results from consolidated-undrained triaxial compression tests showed the
324 strength of fiber-soil mixture superior to strength of natural soil, and that the
325 influence of fibers increases with confining pressures. Fiber-clay samples showed
326 increase in **large displacement** shear strength and fibers restricted the dilatation of
327 soil mixture during undrained shear;
- 328 ● Results from the drained and undrained triaxial tests indicate that the fiber content
329 had a greater influence on the apparent cohesion than on the friction angle. Fiber-
330 clay specimens presented “bulging” behavior after shearing in both drainage and
331 undrained conditions. **Drainage affected the improvement in the shear strength of**
332 **fiber-reinforced soils, with similar improvement in the drained and undrained tests**
333 **for higher confining stresses, and**
- 334 ● The **predictive** model of Jamei et al. (2013) was used to capture the undrained
335 shear strength. Results were found to adequately predict the undrained shear
336 strength of clay-fiber mixtures at low effective stresses but showed deviations at
337 high effective stresses.

339 **Acknowledgments**

340
341 Authors acknowledge the Laboratory of Geotechnics and Geosynthetics of the
342 Federal University of Sao Carlos (UFSCar) and Laboratory of Geotechnics of Federal
343 University of Viçosa (UFV).

346 **References**

- 1
2
3 347 Abou Diab, A., Najjar, S. S., Sadek, S., Taha, H., Jaffal, H., and Alahmad, M. (2018).
4
5 348 “Effect of compaction method on the undrained strength of fiber-reinforced clay.”
6
7 349 *Soils and Foundations*, Elsevier B.V., 58(2), 462–480.
- 8
9
10 350 Abou Diab, A., Sadek, S., Najjar, S., and Abou Daya, M. H. (2016). “Undrained shear
11
12 351 strength characteristics of compacted clay reinforced with natural hemp fibers.”
13
14 352 *International Journal of Geotechnical Engineering*, 10(3), 263–270.
- 15
16
17 353 Anagnostopoulos, C. A., Papaliangas, T. T., Konstantinidis, D., and Patronis, C. (2013).
18
19 354 “Shear Strength of Sands Reinforced with Polypropylene Fibers.” *Geotechnical and*
20
21 355 *Geological Engineering*, 31(2), 401–423.
- 22
23
24 356 ASTM 854-06. (2006). “Standard Test Methods for Specific Gravity of Soil Solids by
25
26 357 Water Pycnometer.” *Astm D854*.
- 27
28
29 358 ASTM ASTM D698 (2012). “Standard Test Methods for Laboratory Compaction
30
31 359 Characteristics of Soil Using Standard Effort (12 400 ft-lbf/ft³ (600 kN-m/m³)).”
32
33 360 *ASTM International*.
- 34
35
36 361 ASTM D2487-17. (2017). “Standard Practice for Classification of Soils for Engineering
37
38 362 Purposes (Unified Soil Classification System), ASTM International, West
39
40 363 Conshohocken, PA, 2017, www.astm.org.” *ASTM Standard Guide*.
- 41
42
43 364 ASTM D4318-10. (2005). “Standard Test Methods for Liquid Limit, Plastic Limit, and
44
45 365 Plasticity Index of Soils.” *Report*.
- 46
47
48 366 ASTM D4452. (2014). “D4452 Standard Practice for X-Ray Radiography of Soil
49
50 367 Samples.”
- 51
52
53 368 ASTM D4767. (2020). “ASTM D4767-11, Standard Test Method for Consolidated
54
55 369 Undrained Triaxial Compression Test for Cohesive Soils, ASTM International, West
56
57 370 Conshohocken, PA, 2011.”

- 1
2
3
4
5
6
7
8
9
10
11
12
13
14
15
16
17
18
19
20
21
22
23
24
25
26
27
28
29
30
31
32
33
34
35
36
37
38
39
40
41
42
43
44
45
46
47
48
49
50
51
52
53
54
55
56
57
58
59
60
61
62
63
64
65
- 371 ASTM D7181. (2020). “D7181 Standard Test Method for Consolidated Drained Triaxial
372 Compression Test for Soils.”
- 373 ASTM D7928-17 (2017). “Standard Test Method for Particle-Size Distribution
374 (Gradation) of Fine-Grained Soils Using the Sedimentation (Hydrometer) Analysis.”
375 *ASTM International, West Conshohocken, PA.*
- 376 Attom, M. F., and Al-Tamimi, A. K. (2010). “Effects of polypropylene fibers on the shear
377 strength of sandy soil.” *International Journal of Geosciences*, 01(01), 44–50.
- 378 Consoli, N. C., Montardo, J. P., Marques Prietto, P. D., and Pasa, G. S. (2002).
379 “Engineering behavior of a sand reinforced with plastic waste.” *Journal of*
380 *Geotechnical and Geoenvironmental Engineering*, 128(6), 462–472.
- 381 Li, C. (2005). “Mechanical response of fiber-reinforced soil.” PhD dissertation,
382 University of Texas at Austin, Austin, TX, (USA), 190p.
- 383 Diambra, A., and Ibraim, E. (2014). “Modelling of fibre–cohesive soil mixtures.” *Acta*
384 *Geotechnica*, 9(6), 1029–1043.
- 385 Ehrlich, M., Almeida, S., Curcio, D., Almeida, M. S. S., Curcio, D., Almeida, S., Curcio,
386 (2019). “Hydro-mechanical behavior of a lateritic fiber-soil composite as a waste
387 containment liner.” *Geotextiles and Geomembranes*, Elsevier, 47(1), 42–47.
- 388 Ekinci, A., and Ferreira, P. M. V. (2012). “The undrained mechanical behaviour of a
389 fibre-reinforced heavily over- consolidated clay.” Proceedings: ISSMGE Technical
390 Committee TC 211 International Symposium on Ground Improvement (IS-GI
391 BRUSSELS 2012), May, 2012.
- 392 Feuerharmel, M. R. (2000). “Comportamento de Solos Reforçados com Fibras de
393 Polipropileno.” Universidade Federal do Rio Grande do Sul (UFRGS), Porto Alegre
394 (RS), 152 p., 2000 (in portuguese).
- 395 Freilich, B. J. J., Li, C., and Zornberg, J. G. G. (2010). “Effective shear strength of fiber-

- 396 reinforced clays.” *9th International Conference on Geosynthetics - Geosynthetics:*
 397 *Advanced Solutions for a Challenging World, ICG 2010, (Icd), 1997–2000.*
- 398 Futai, M. M., Almeida, M. S. S., Lacerda, W. A. “Yield, Strength, and Critical State
 399 Behavior of a Tropical Saturated Soil”. *Journal of Geotechnical and*
 400 *Geoenvironmental Engineering, 2004.*
- 401 Gelder, C., and Fowmes, G. J. (2016). “Mixing and compaction of fibre- and lime-
 402 modified cohesive soil.” *Proceedings of the Institution of Civil Engineers: Ground*
 403 *Improvement, 169(2), 98–108.*
- 404 Gray, D. H., T. A.-R. (1986). “Behavior of fabric- versus fiber-reinforced sand.” 112(8),
 405 804–820.
- 406 Hamidi, A., and Hooresfand, M. (2013). “Effect of fiber reinforcement on triaxial shear
 407 behavior of cement treated sand.” *Geotextiles and Geomembranes, Elsevier Ltd,*
 408 36(0), 1–9.
- 409 Hejazi, S. M., Sheikhzadeh, M., Abtahi, S. M., and Zadhoush, A. (2012). “A simple
 410 review of soil reinforcement by using natural and synthetic fibers.” *Construction and*
 411 *Building Materials, Elsevier Ltd, 30, 100–116.*
- 412 Jamei, M. . V. P. and G. H. (2013). “Shear failure criterion based on experimental and
 413 modeling results for fiber-reinforced clay.” *Int. J. Geomech., 13(6), 882–893.*
- 414 Khatri, V. N., Dutta, R. K., Venkataraman, G., and Shrivastava, R. (2016). “Shear
 415 strength behaviour of clay reinforced with treated coir fibres.” *Periodica*
 416 *Polytechnica Civil Engineering, 60(2), 135–143.*
- 417 Kumar, P., and Singh, S. P. (2008). “Fiber-reinforced fly ash subbases in rural roads.”
 418 *Journal of Transportation Engineering, 134(4), 171–180.*
- 419 Li, C., and Zornberg, J. G. (2005). “Interface shear strength in fiber-reinforced soil.”
 420 *Proceedings of the 16th International Conference on Soil Mechanics and*

- 421 *Geotechnical Engineering: Geotechnology in Harmony with the Global*
 422 *Environment*, 3, 1373–1376.
- 423 Li, C., and Zornberg, J. G. (2013). “Mobilization of reinforcement forces in fiber-
 424 reinforced soil.” *Journal of Geotechnical and Geoenvironmental Engineering*,
 425 139(1), 107–115.
- 426 Louzada, N. dos S. L., Malko, J. A. C., and Casagrande, M. D. T. (2019). “Behavior of
 427 Clayey Soil Reinforced with Polyethylene Terephthalate.” *Journal of Materials in*
 428 *Civil Engineering*, 31(10), 04019218.
- 429 Ma, Q., Yang, Y., Xiao, H., and Xing, W. (2018). “Studying shear performance of flax
 430 fiber-reinforced clay by triaxial test.” *Advances in Civil Engineering*, 2018.
- 431 Maheshwari, K., Desai, A. K., and Solanki, C. H. (2011). “Application and modeling of
 432 fiber reinforced soil.” *Indian Geotechnical Conference IGC*, 497–500.
- 433 Michalowski, and Zhao. (1996). “Failure of fiber-reinforced granular soils.” *Journal of*
 434 *Geotechnical Engineering*, 122(March), 226–234.
- 435 Mirzababaei, M., Anggraini, V., and Haque, A. (2020). “X-ray computed tomography
 436 imaging of fibre-reinforced clay subjected to triaxial loading.” *Geosynthetics*
 437 *International*, 27(6), 635–645.
- 438 Mirzababaei, M., Arulrajah, A., Horpibulsuk, S., and Aldava, M. (2017). “Shear strength
 439 of a fibre-reinforced clay at large shear displacement when subjected to different
 440 stress histories.” *Geotextiles and Geomembranes*, Elsevier Ltd, 45(5), 422–429.
- 441 Mirzababaei, M., Miraftab, M., Mohamed, M., and McMahon, P. (2013). “Unconfined
 442 compression strength of reinforced clays with carpet waste fibers.” *Journal of*
 443 *Geotechnical and Geoenvironmental Engineering*, 139(3), 483–493.
- 444 Mirzababaei, M., Mohamed, M., A. Arulrajah, A.; Horpibulsuk, S. and Anggraini, V.
 445 (2018). “Practical approach to predict the shear strength of fibre-reinforced clay.”

- 446 *Geosynthetics International*, 25(1).
- 1
2 447 Murray, J. J., Frost, J. D., and Wang, Y. (2000). "Behavior of a sandy silt reinforced with
3
4 448 discontinuous recycled fiber inclusions." *Transportation Research Record*, (1714),
5
6
7 449 9–17.
- 8
9 450 Najjar, S. S., Sadek, S., and Alcovero, A. (2013). "Quantification of model uncertainty in
10
11 451 shear strength predictions for fiber-reinforced sand." *Journal of Geotechnical and*
12
13 452 *Geoenvironmental Engineering*, 139(1), 116–133.
- 14
15
16 453 Özkul, Z. H., and Baykal, G. (2007). "Shear behavior of compacted rubber fiber-clay
17
18 454 composite in drained and undrained loading." *Journal of Geotechnical and*
19
20 455 *Geoenvironmental Engineering*, 133(7), 767–781.
- 21
22
23 456 Palat, A, Roustaei, M, Hendry, M. T. (2019). "Effect of fiber content on the mechanical
24
25 457 behavior of fiber-reinforced clay, *Proceedings of 72nd Canadian Geotechnical*
26
27 458 *Conference - Geo St. John's, Newfoundland and Labrador, Canada, October 2, 2019.*
- 28
29
30 459 Plé, O., and Lê, T. N. H. H. (2012). "Effect of polypropylene fiber-reinforcement on the
31
32 460 mechanical behavior of silty clay." *Geotextiles and Geomembranes*, 32(0), 111–116.
- 33
34 461 Prabakar, J., and Sridhar, R. S. (2002). "Effect of random inclusion of sisal fibre on
35
36 462 strength behaviour of soil." *Construction and Building Materials*, 16(2), 123–131.
- 37
38
39 463 Rowland Otoko, G. (2014). "Stress – Strain Behaviour of an Oil Palm Fibre Reinforced
40
41 464 Lateritic Soil." *International Journal of Engineering Trends and Technology*, 14(6),
42
43 465 295–298.
- 44
45
46 466 Sadek, S., Najjar, S. S., and Freiha, F. (2010). "Shear strength of fiber-reinforced sands."
47
48 467 *Journal of Geotechnical and Geoenvironmental Engineering*, 136(3), 490–499.
- 49
50
51 468 Santoni, B. R. L., Tingle, J. S., Members, A., and Webster, S. L. (2001). "Engineering
52
53 469 properties of sand-fiber mixtures for road construction." *J. Geotech. Geoenviron.*
54
55 470 *Eng.*, (March), 258–268.
- 56
57
58
59
60
61
62
63
64
65

- 1
2
3
4
5
6
7
8
9
10
11
12
13
14
15
16
17
18
19
20
21
22
23
24
25
26
27
28
29
30
31
32
33
34
35
36
37
38
39
40
41
42
43
44
45
46
47
48
49
50
51
52
53
54
55
56
57
58
59
60
61
62
63
64
65
- 471 Shukla, S. K. (2017). *Fundamentals of Fibre-Reinforced Soil Engineering. Developments*
472 *in Geotechnical Engineering.*
- 473 Skempton, A. W. (1954). “The pore-pressure coefficients a and b.” *Geotechnique*, 4(4),
474 143–147.
- 475 Sotomayor, J. M. G., and Casagrande, M. D. T. (2018). “The performance of a sand
476 reinforced with coconut fibers through plate load tests on a true scale physical
477 model.” *Soils and Rocks*, 41(3), 361–368.
- 478 Suffri, N., Jeludin, M., and Rahim, S. (2019). “Behaviour of the Undrained Shear Strength
479 of Soft Clay Reinforced with Natural Fibre.” *IOP Conference Series: Materials*
480 *Science and Engineering*, 690(1).
- 481 Tang, C., Shi, B., Gao, W., Chen, F., and Cai, Y. (2007). “Strength and mechanical
482 behavior of short polypropylene fiber reinforced and cement stabilized clayey soil.”
483 *Geotextiles and Geomembranes*, 25(3), 194–202.
- 484 Trindade, T. P. da, Iasbik, I., Lima, D. C. de, Minette, E., Silva, C. H. de C., Carvalho, C.
485 A. B. de, Bueno, B. de S., and Machado, C. C. (2006). “Estudos laboratoriais do
486 comportamento de um solo residual arenoso reforçado com fibras de polipropileno,
487 visando à aplicação em estradas florestais.” *Revista Árvore*, 30(2), 215–222.
- 488 Velloso, R. Q., M. D. T. Casagrande, E. A. Vargas Junior and N. C. C. 2012. (2010).
489 “Simulation of the mechanical behavior of fiber reinforced sand using the discrete
490 element method.” *Soils and Rocks*, 33(2), 81–93.
- 491 Wu, Y., Li, Y., and Niu, B. (2014). “Assessment of the mechanical properties of sisal
492 fiber-reinforced silty clay using triaxial shear tests.” *The Scientific World Journal*,
493 2014.
- 494 Xu, Y., Wu, S., Williams, D. J., and Serati, M. (2018). “Determination of peak and
495 ultimate shear strength parameters of compacted clay.” *Engineering Geology*,

496 Elsevier, 243(April), 160–167.

497 Ziegler, S., Leshchinsky, D., Ling, H. I., and Perry, E. B. (1998). “Effect of short

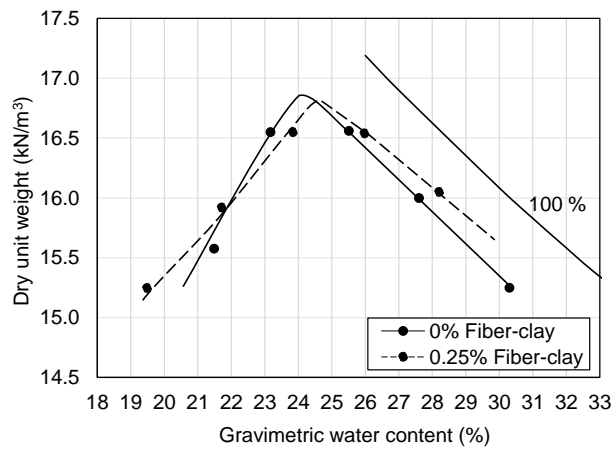
498 polymeric fibers on crack development in clays.” *Soils and Foundations*, Japanese

499 Geotechnical Society, 38(1), 247–253.

500

501

FIGURES



502

Fig. 1. Standard Proctor compaction curves for clayey soil with fiber contents of 0 and 0.25%.

503

504

505

506

507

508

509

510

511

512

513

514

515

516

517

518

519

520

521

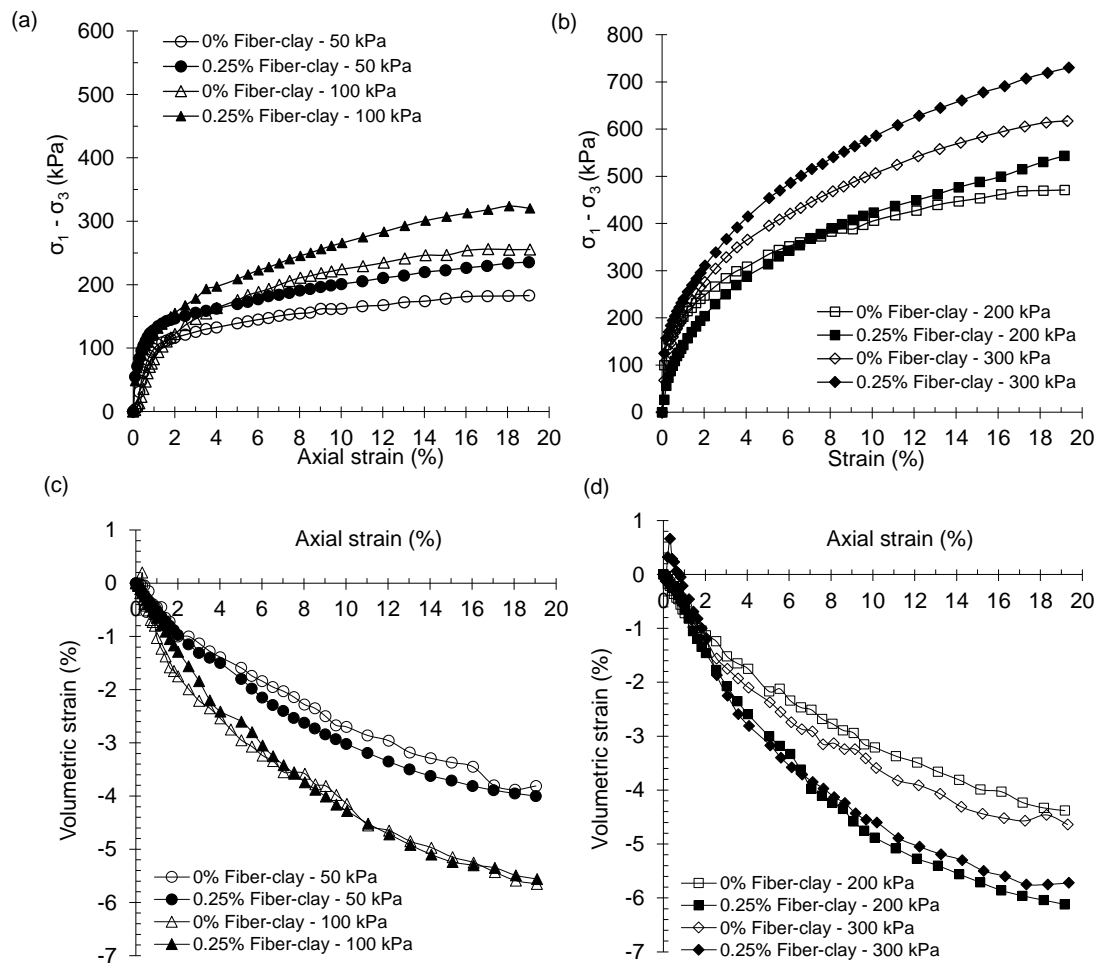


Fig. 2. Results from CD triaxial tests: (a) Deviator stress-strain curves for mean effective stresses of 50 and 100 kPa; (b) Deviator stress-strain curves for mean effective stresses of 200 and 300 kPa; (c) Volumetric strain-axial strain curves for mean effective stresses of 50 and 100 kPa; (d) Volumetric strain-axial strain curves for mean effective stresses of 200 and 300 kPa.

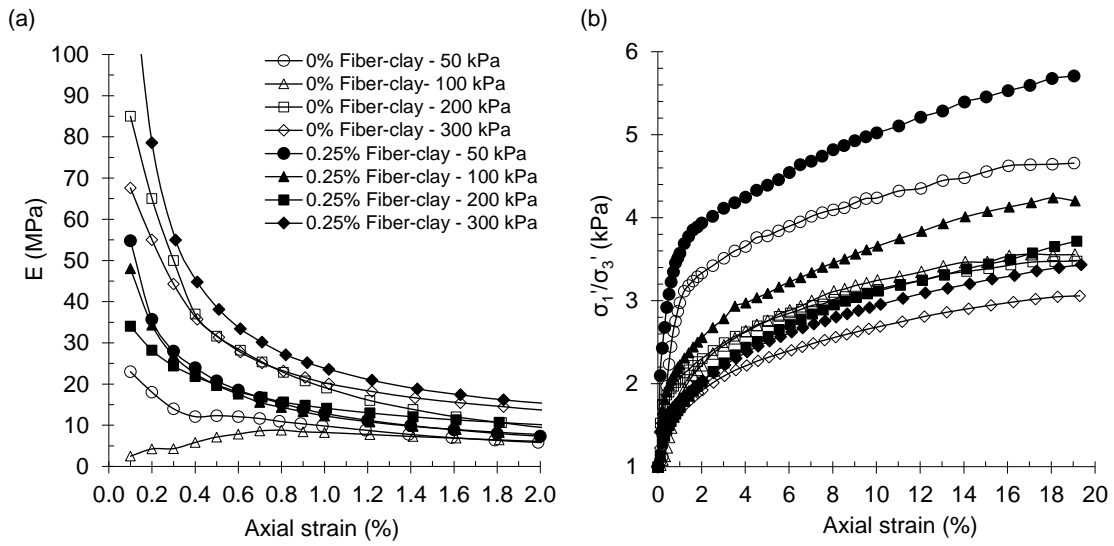
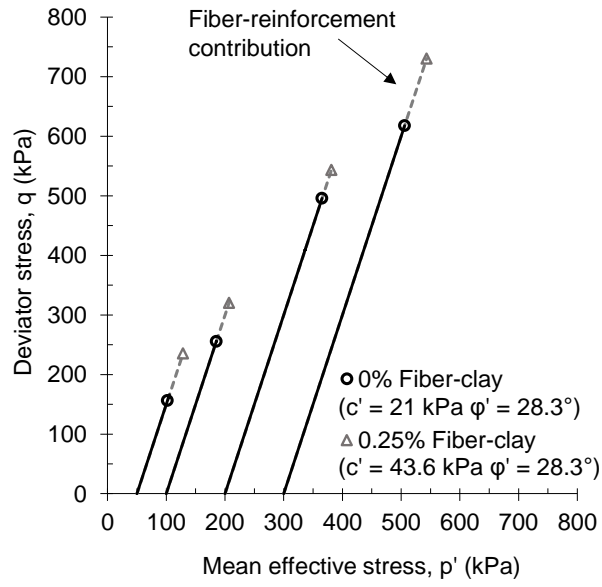


Fig. 3. Results of CD triaxial tests for natural and PP fiber-clay: (a) secant modulus; (b) σ_1'/σ_3' .

1
2
3
4
5
6
7
8
9
10
11
12
13
14
15
16
17 529
18
19 530
20
21 531
22
23 532
24
25 533
26
27 534
28
29 535
30
31 536
32
33 537
34
35 538
36
37 539
38
39 540
40
41 541
42
43 542
44
45 543
46
47 544
48
49 545
50
51 546
52
53 547
54
55 548
56
57 549
58
59
60
61
62
63
64
65



550

551 **Fig. 4.** Stress paths and effective shear strength parameters from CD triaxial tests on clayey soil with fiber
 552 contents of 0 and 0.25%.

553

554

555

556

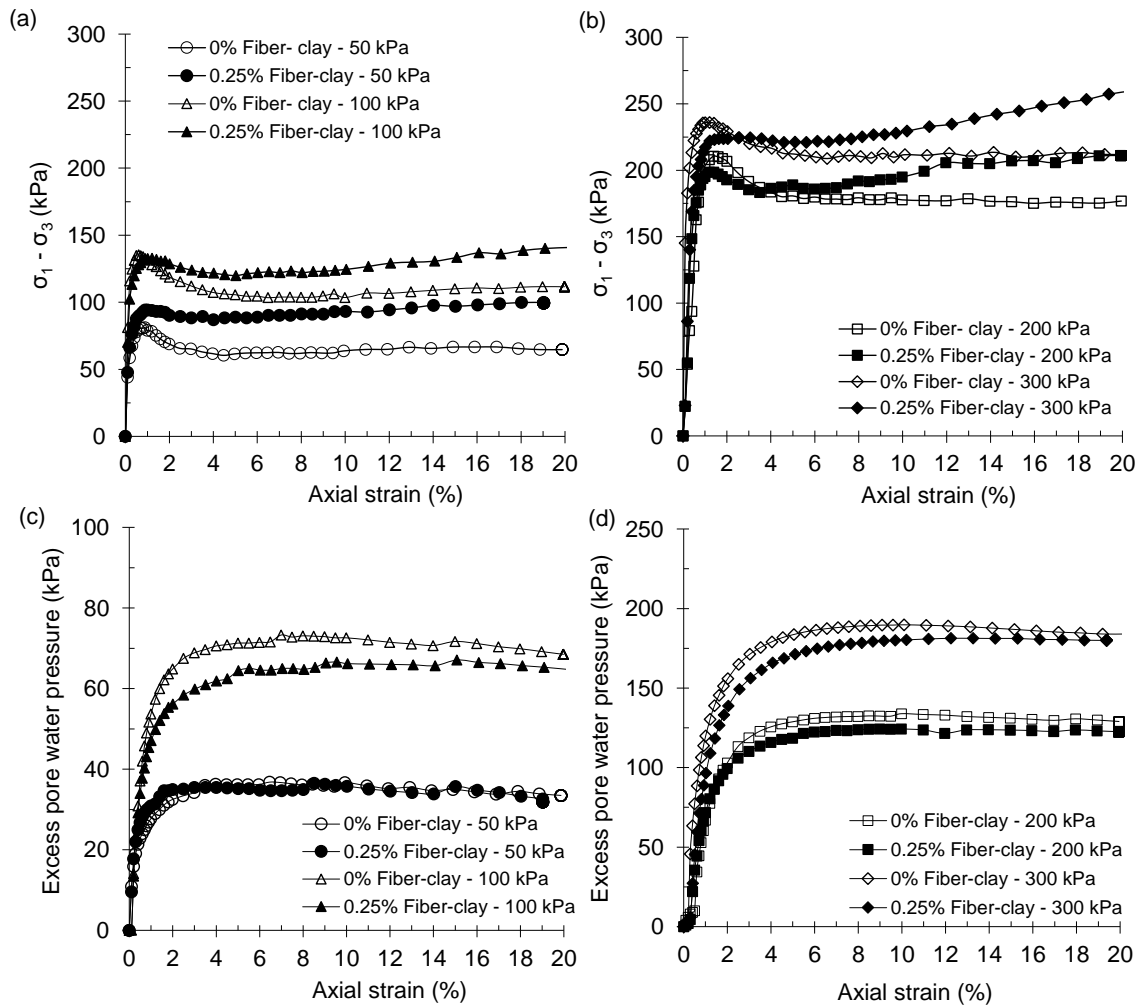


Fig. 5. Results from CU triaxial tests: (a) Stress-strain curves for confining stresses of 50 and 100 kPa; (b) Stress-strain curves for confining stresses of 200 and 300 kPa; (c) Pore-water pressure for confining stresses of 50 and 100 kPa; (d) Pore-water pressure for confining stresses of 200 and 300 kPa.

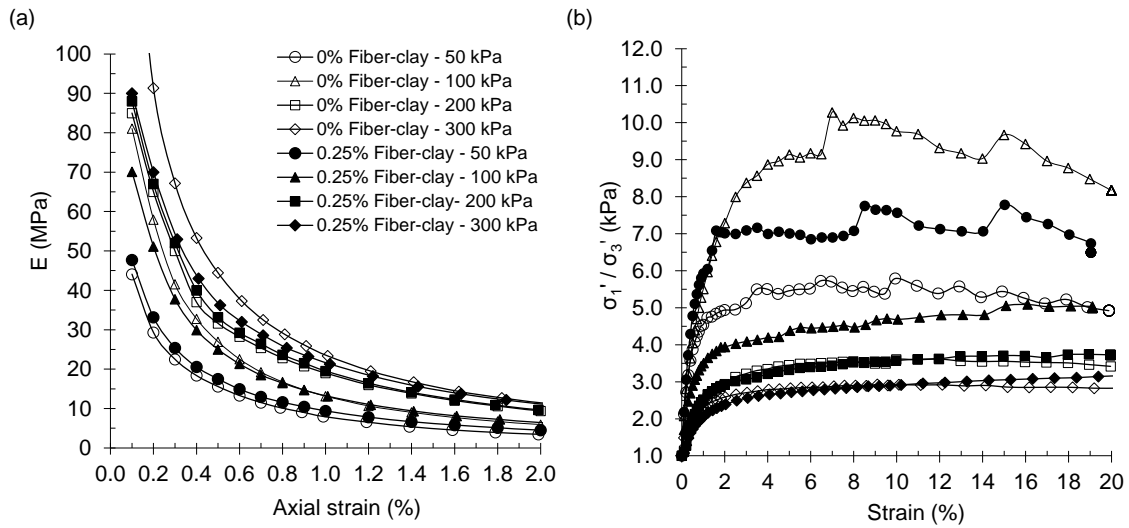
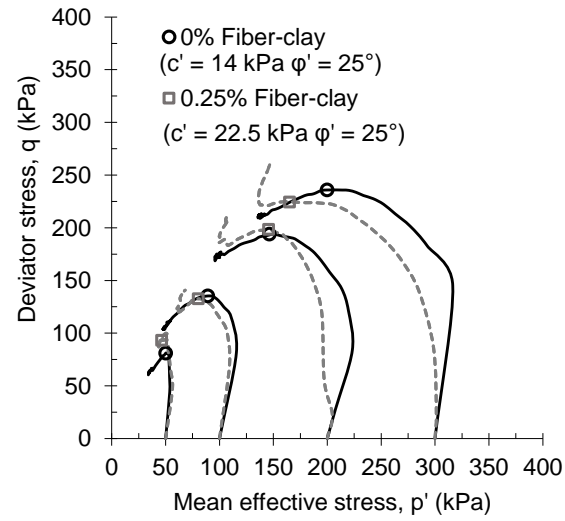


Fig. 6. Results from CU triaxial tests for natural and PP fiber-clay mixtures: (a) Initial stiffness; (b) σ_1' / σ_3' .



582

583 **Fig. 7.** Stress paths and effective shear strength parameters from CU triaxial tests on clayey soil with fiber

584 contents of 0 and 0.25%

585

586

587

588

589

590

591

592

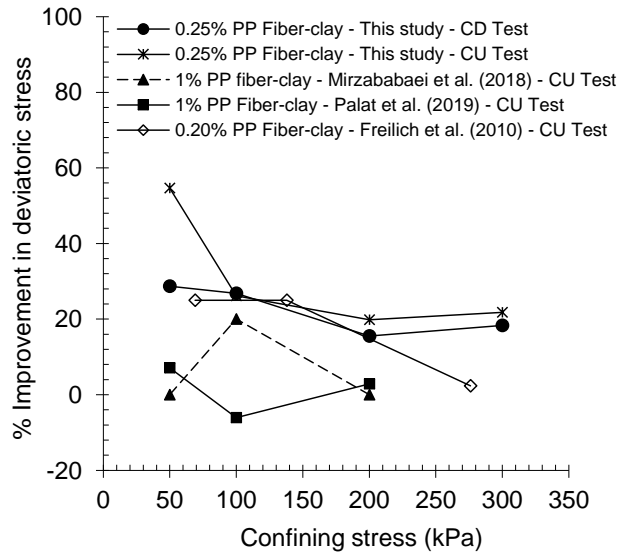
593

594

595

596

597



598

599 **Fig. 8.** Improvement in peak deviator stresses observed in this study with other CD triaxial test results from
 600 the literature.

601

602

603

604

605

606

607

608

609

610

611

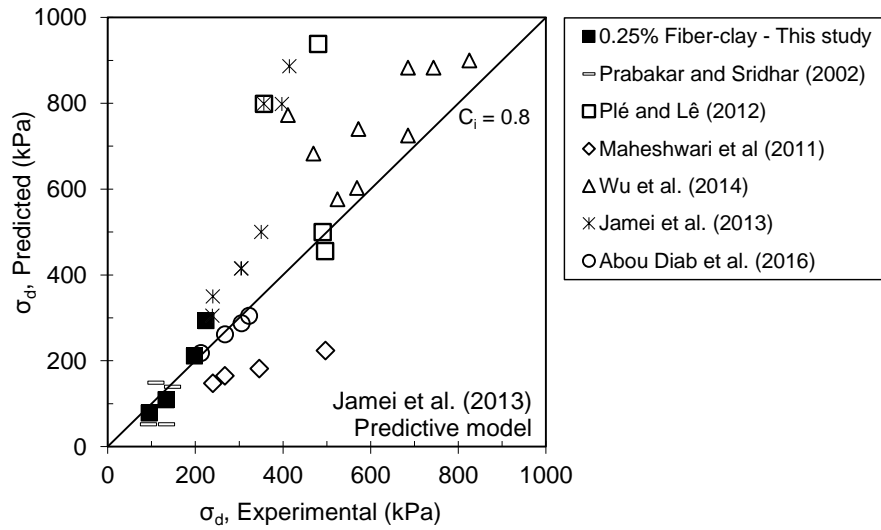


Fig. 9. Comparison of undrained shear strength values at failure from the CU triaxial tests performed at different confining stresses with predictions from the model of Jamei et al. (2013).

634

TABLES

635 **Table 1.** Parameters of the model of Jamei et al. (2013) for the soil tested in this study.

PP fiber content (%)	L_f (m)	d_f (m)	$\chi_{F,v}$ (%)	σ_3 (kPa)	σ'_3 (kPa)	σ_d Measured (kPa)	c' (kPa)	ϕ' (°)
				50	23.1	81.1		
0	-	-	-	100	44.0	131.0	14	25
				200	81.6	193.9		
				300	117.6	235.9		
				50	19.6	94.2		
0.25%	0.012	0.000396	0.48	100	36.1	132.7	-	-
				200	73.4	197.6		
				300	101.2	223.8		

636